EUROPEAN GROUND MOTION SERVICE FOR BRIDGE MONITORING: TEMPORAL AND THERMAL DEFORMATION CROSS-CHECK USING COSMO-SKYMED INSAR

R. Eskandari *, M. Scaioni

Dept. of Architecture, Built Environment and Construction Engineering, Politecnico di Milano via Ponzio 31, 20133 Milano, Italy - rasoul.eskandari@polimi.it, marco.scaioni@polimi.it

KEY WORDS: European Ground Motion Service (EGMS), Synthetic Aperture Radar (SAR), InSAR, Persistent Scatterer Interferometry (PSI), Bridge, Deformation Monitoring, Thermal Dilation

ABSTRACT:

This paper elaborates on the potential of the deformation time-series provided by European Ground Motion Service (EGMS) data points for bridge monitoring, in terms of the response of bridge structures to temporal and thermal deformations. For this purpose, high-resolution Cosmo-SkyMed (CSK) Synthetic Aperture Radar (SAR) images have been utilized through Persistent Scatterer SAR Interferometry (PS-InSAR) to derive spatially detailed deformation time-series of two bridges located at the north of Lombardy region, Italy. Then, the Annual Displacement Velocity and Thermal Expansion Coefficient of the data points in both datasets are extracted based on the corresponding deformation time-series. The response parameters are post-processed through projection and compensation steps to become comparable. Cross-checking the results by comparing the response parameters along the bridges showed that the global (for L3 products) and local (for L2b products) differential behaviour and the variation of the values of these parameters from one side to the other side of each bridge are consistent between CSK and EGMS datasets. However, the EGMS L3 information shows a slightly lower magnitude in both displacement velocity and thermal expansion coefficient responses. According to the revealed capability of EGMS information in this work, it can be concluded that the EGMS data points, if spatially cover a bridge, can present a reasonable and sufficient insight into the temporal evolution of displacement and thermal structural response, suitable for structural health monitoring and condition assessment of bridges under operational and environmental loads.

1. INTRODUCTION

Bridges, as a principal element of transport infrastructures, are essentially contributing to the service quality and development of urban areas. Due to a variety of geo-environmental factors and operational loads, bridges are subjected to inevitable degradation and strength attenuation during their lifetime (Sun et al., 2020; Wang et al., 2021). Therefore, monitoring of health and operational status of these assets, with high levels of systemic vulnerability, is an essential need for planning rehabilitation and/or damage prevention measures. Structural deformation can be considered an effective indicator for condition assessment and evaluation of inherent damages (Tang et al., 2022). Measuring this quantity is a special branch of Structural Health Monitoring (SHM) using different techniques.

In-situ measurements and close-range remote sensing, such as attached-to-structure Linear Variable Differential Transducers (LVDT) (Mayunga et al., 2021), Geodetic Levelling (e.g. using Robotic Total Station (Zainon and Fong Kian, 2021)), Terrestrial Laser Scanning (TLS) (Gawronek and Makuch, 2019), and Global Navigation Satellite System (GNSS) with installed stations (Xi et al., 2021), are providing valuable information on structural deformation with varying accuracy and availability. As far as short-term in-situ tests are concerned, these technologies are essential to be implemented (Zarate Garnica et al., 2022). However, these techniques are considered to be expensive and time-consuming approaches for deformation monitoring purposes, particularly in the case of long-term measurements.

On the other hand, Satellite-borne Remote Sensing techniques are providing practical tools for the assessment of the operational state of infrastructures. Satellite-borne Synthetic Aperture Radar (SAR) Interferometry (InSAR) is a promising radar remote sensing technique which has been used for infrastructure deformation monitoring during the last decades (Macchiarulo et al., 2022b). Using Multi-Temporal (MT) SAR images, the advanced Differential Interferometric SAR (DInSAR) approaches can provide millimetric-level precision of deformation time-series for sensor-friendly targets, so-called Persistent Scatterer (PS), on the ground surface, usually sensed over built environments. The potential and technical aspects of InSAR for bridge monitoring are examined by several works (Lazecky et al., 2015; Selvakumaran et al., 2021).

Different satellite SAR missions provide different temporal and spatial resolutions (with almost global spatial coverage and varying temporal coverage depending on the operational lifetime), suitable for current or retrospective assessment of the health status of bridges in different scales.

For instance, freely available C-band SAR images acquired by ERS (temporal coverage 1992-2001) and Sentinel-1 (temporal coverage 2014-ongoing) provide ~30m and ~20m spatial resolution, respectively. In the case of the application of low to medium-resolution ERS and Envisat SAR images for bridge monitoring, it has been reported that the number of PSs may not be sufficient to assess the bridges (Poreh et al., 2016), and they are likely to be useful for analysing the surrounding area to have a general overview concerning the possible causes of the deformations imposed on the bridge, such as subsidence or mining-related displacements (Lazecký et al., 2014). However, it has been shown that processing of the Sentinel-1 SAR images through an improved MT-DInSAR can provide valuable information of bridge monitoring in a large scale (Macchiarulo et al., 2022a).

Commercial products of Italian Cosmo-SkyMed (CSK) and German TerraSAR-X (temporal coverage 2010-ongoing) missions offer images with 3m (HIMAGE mode) up to 1m

* Corresponding author

(Spotlight mode) spatial resolution. Due to their high-resolution capability, they have been extensively used to detect the deformation time-series of multiple natural targets on different types of linear infrastructure, especially bridges (Gagliardi et al., 2022; Caspani et al., 2023).

The European Ground Motion Service (EGMS), as an essential section of the Copernicus Land Monitoring Service (CLMS) framework, provides a freely-accessible continent-wide database of information regarding ground deformation almost all over Europe (Crosetto et al., 2020; Costantini et al., 2022). The project, which has been carried out by Sentinel-1 InSAR processing, has brought the opportunity for different monitoring purposes, such as geo-hazard assessment and urban area and infrastructure monitoring. Regardless of the exceptional temporal nominal resolution of 12 and 6 days, respectively for "Calibrated" and "Ortho" products (will be discussed in Section 2), the uniform grid of the available data points in "Ortho" products presents a 100m spatial resolution, while the "Calibrated" products introduce the real sparse processed targets of Sentinel-1 SAR images.

In this work, the potential of EGMS datasets for bridge monitoring is evaluated. It has been done through a cross-checking of *Displacement Velocity* and *Thermal Dilation* parameters using high-resolution CSK SAR images. Due to the low spatial resolution of the EGMS uniform grid, and the deformation time-series being averaged based on nearby InSAR targets in "Ortho" products, it is essential to assess the applicability of this data, especially for bridges.

2. STUDY AREA AND MATERIALS

2.1 Case Study

The case studies of this work are two bridges located in the southern area of Lecco Province, northern Italy: 1) a multi-span continuous bridge hosting a railway line, with a total length of ~120m, and 2) a cable-stayed road bridge with a total length of ~220m. The bridges pass the Adda River supplied by the Lake of Como. This area, particularly the lakeshore urban areas such as Como town, is significantly affected by different levels of ground motion during past years, and it has been of great interest for several researchers to investigate the ground displacement phenomenon in the area using ground-based measurements and satellite-borne InSAR data in different scales (Nappo et al., 2020; Eskandari and Scaioni, 2023a, b). Figure 1 shows the area of interest (red square) in northern Italy, containing two bridges under study.

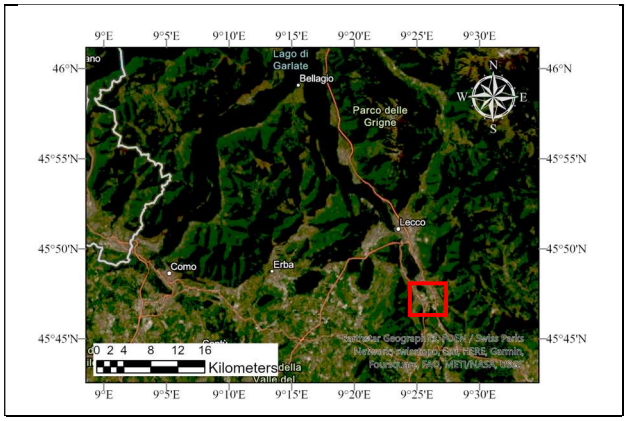

Figure 1. Area of interest: Adda River, the right-side branch of Como Lake, North of Italy.

2.2 EGMS Products

European Ground Motion Service (EGMS) provides land surface displacement time-series in different levels of products. "Basic" products are the first level of deformation time-series along the Line- of Sight (LOS) direction (i.e., satellite incident angle w.r.t nadir), available for a sparse grid of points for both Ascending (ASC) and Descending (DSC) acquisition geometry. The measurements are relative with respect to a local Reference Point (RP). "Calibrated" and "Ortho" are other types of products accessible through the EGMS portal, which are used in this study with the characteristics summarized in Table 1. Both datasets are not relative to a local RP, instead, the measurements are calibrated using a uniform grid of GNSS data over Europe, as prior information on 3D deformations.

Regarding the temporal resolution, "Calibrated" data presents a nominal 12-day revisit time for each ASC and DSC dataset; however, for "Ortho" products, this resolution has been increased to 6-day due to the fact ASC and DSC datasets are combined to obtain UP-Down and East-West displacements. On the other hand, the "Calibrated" products are available on a sparse grid of the true measurement points of Sentinel-1SAR images processed through InSAR analysis, while the "Ortho" datapoints are presented on a uniform 100m grid.

The spatial coverage of EGMS datapoints is almost all over Europe, and the temporal coverage, up to the date of this paper, is February 2015-December 2021 and January 2016-December 2021 for "Calibrated" and "Ortho" products, respectively. To have a consistent time span, only the time-series obtained in January 2016-December 2021 are chosen for this study. For more details on the type of products and the implemented algorithm for obtaining this valuable information, refer to (Ferretti et al., 2021; Kotzerke et al., 2022).

Table 1. Description of EGMS products used in this study.

Product	"Calibrated L2b"	"Ortho L3"
Direction	LOS DSC (Incident Angle 33.66°)	Up-Down & East-West
Datapoints	Sparse (Sentinel-1 InSAR points)	Uniform Grid (100 m)
Temporal Coverage	09-Jan-2016 – 20-Dec-2021	05-Jan-2016 – 16-Dec-2021
Time for Temperature	05:00:00 A.M.	Mean Daily Temperature

2.3 Cosmo-SkyMed Data

To use the Cosmo-SkyMed (CSK) InSAR measurements for the cross-checking purpose followed in this study, 99 CSK images are used to obtain the deformation time-series over the study area. The characteristics of the CSK images used in this study are outlined in Table 2.

Table 2. Cosmo-SkyMed data characteristics

Geometry	Descending
Incident Angle	26.57°
Temporal Coverage	21-Jan-2016 – 04-Dec-2021
Time for Temperature	05:00:00 A.M.

2.4 InSAR and Post-Processing Auxiliary Data

Digital Elevation Model (DEM) is an important external data for InSAR processing. DEM is used for co-registration purposes, Ground Control Point (GCP) automatic selection, and ground component removal through the Differential InSAR (DInSAR) processing of CSK SAR images. The DEM utilized in this study is DTM 5×5 provided by Lombardy Region Geoportal (available online).

Temperature data are useful to model the effect of temperature on differential phases through DInSAR. Also, the temperature data are used in this study to carry out the displacement-temperature regression analysis to obtain the thermal expansion coefficient of each datapoint. The temperature data of the area containing two bridges under study are obtained at the time of each satellite acquisition (both CSK and Sentinel-1) through VCWDtool (Eskandari and Scaioni, 2023c), a tool for automatic downloading of weather data, including temperature at the satellite acquisition time.

3. METHODOLOGY

The general framework of this work is: *i)* obtaining the deformation time-series for available data points in EGMS L2b (calibrated products from descending orbit track), EGMS L3 (ortho products obtaining vertical and horizontal direction), and CSK InSAR dataset; *ii)* Pre-processing of time-series: Compensation for a same Reference Point (RP) and Projection of time-series on a same direction; *iii)* Post-processing: determination of Displacement velocity [mm/year] and Thermal Expansion Coefficient [mm/°C] through fitting and regression analysis; and *iv)* comparison of these structural parameters obtained from three different datasets along each two bridge. Each part will be discussed in detail in the following sub-sections, and the algorithm and utilized mathematical models are presented.

3.1 CSK InSAR Processing

The superiority of EGMS data is that it provides geocoded and processed data regarding ground deformation time-series using Sentinel-1 InSAR, easily accessible by the corresponding portal. However, in the case of CSK SAR images, they need to be pre-processed and processed through the DInSAR framework to obtain land surface deformation time-series.

In this work, the SARPROZ software package (Perissin et al., 2011), a powerful software for SAR and InSAR processing for several applications, has been used to obtain the time-series from CSK images. First, 99 CSK images have been cropped to the area of interest, and then, co-registered. Instead of using a full-resolution perspective, the pixels considered as the Local Maxima (LM) of backscattering echoes of SAR images are chosen as the initial set of sensor-friendly targets on the objects and land surface, based on the generated reflectivity (mean amplitude) map using Multi-Temporal (MT) SAR images. Also, the Amplitude Stability Index ($I_{AmpStab}$) map is generated considering MT SAR images. Considering a Minimum Spanning Tree (MST) image connection configuration, the interferograms are produced, and the spatial coherence γ_{sp} of the pixels have been calculated (Eskandari, 2022).

Among the initially selected pixels, Persistent Scatterers (PSs), i.e., pixels with high quality of amplitude and phase components, have been selected according to the criterion of

$$(I_{AmpStab} + \gamma_{sp}) > 1 \tag{1}$$

The value of $I_{AmpStab}$ and γ_{sp} may vary in the interval of $[-Inf, 1]$ and [0,1], which shows that the formula in Equation 1 can vary in the interval of $[-Inf, 2]$. By involving the contributions from both amplitude and phase components of SAR images, this joint parameter allows a more accurate selection of PS Candidates (PSCs) for MT-InSAR processing.

Atmospheric artefacts result in a component in DInSAR formulation which need to be estimated and removed in the final estimation of useful parameters. To estimate this portion of spatial differential phases, a sparser representation of selected PSC is selected, which is spatially connected with Delaunay triangulation, to perform MT-DInSAR processing for each connection, considering a single-master configuration of image connections. The sparser representation selection is due to the fact that the atmospheric delay variation is negligible in short distances (while a great level of temporal variations can be seen), so there is no need to establish PS connections in a dense network of PSCs.

After estimation of Atmospheric Phase Screens described above, the PSCs are processed through MT-InSAR non-linear analysis with respect to a selected RP, to obtain: 1) deformation time-series, 2) residual height of the target w.r.t the imported DEM, and 3) thermal variation model. Instead of considering a linear hypothesis (which results in a global deformation trend [mm/year]), the non-linear deformation analysis (Ferretti et al., 2000) is performed here to reveal the actual deformation of each target and to detect any kind of abnormalities in deformations time-series. Temporal Coherence (γ_{temp}), assigned to each processed PSC, is one of the technical outcomes of MT-DInSAR processing which shows the overall quality of the parameter estimation, and it is representative of the amount of phase residuals after model estimation. Thresholding the value of this parameter (which varies between 0 and 1) is a reliable criterion for choosing the final PSs among processed PSC. This criterion is adopted in this study for the final PSs selection.

3.2 Time-series Compensation and Projection

Since the EGMS L2b and L3 products are calibrated concerning prior information on land surface deformation based on GNSS measurements, the time-series are not relative to a specific RP. On the other hand, CSK measurements are introduced based on an RP in the area of analysis. To tackle this discrepancy, an EGMS L3 point at the southern part of the area is considered as RP_{L3}, and the closest points of EGMS L2b and CSK datasets to RP_{L3} are considered as the RP_{L2b} and RP_{CSK}, respectively. Then, all the time-series of each dataset are compensated with respect to the corresponding reference point as

$$\left\{TS_1^{i,j}, \dots, TS_M^{i,j}\right\}_{compens} = \left\{TS_1^{i,j}, \dots, TS_M^{i,j}\right\}_{orig} - \left\{TS_1^{RP_i}, \dots, TS_M^{RP_i}\right\} \tag{2}$$

where $\left\{TS_1^{i,j}, \dots, TS_M^{i,j}\right\}$ represents the time-series of j^{th} datapoints in dataset i, $\left\{TS_1^{RP_i}, \dots, TS_M^{RP_i}\right\}$ shows the time-series of RP in dataset i. It should be noted that in Equation 2, $i \in \{CSK\ ,\ EGMS\ L2b\ ,\ EGMS\ L3\}$, $j = 1, \dots, N$ where N is the total number of datapoints in each dataset, and M is the total number of SAR images in each dataset.

Projection of the estimated structural parameters along the same direction is essentially needed for multi-sensor comparison purposes. The EGMS L3 product contains two separated datasets: vertical (Up-Down) and horizontal (East-West), while the measurements of EGMS L2b are along LOS DSC L2b (33.66° w.r.t nadir). Also, the CSK measurements are along the LOS direction of CSK satellite acquisition (26.57° w.r.t nadir).

Since, in this study, only descending geometry of EGMS "Calibrated L2b" and CSK is used, it is not possible to retrieve the actual vertical-horizontal components (combining with ascending dataset in a multi-track approach). Here, the LOS CSK is considered as the Reference Direction (RD), and the estimated structural parameters (described in the next sub-section) from both EGMS datasets are projected on this reference direction. The magnitude of parameter $k \in$ {Displacement Velocity v, Thermal Expansion Coefficient α}, can be obtained for EGMS L2b as:

$$\left|\boldsymbol{P}_{RD}^{j,k}\right| = \left|\boldsymbol{P}_{L2b}^{j,k}\right| \cos \Delta\emptyset \tag{3}$$

where $\left|\boldsymbol{P}_{L2b}^{j,k}\right|$ presents the magnitude of parameter k along the LOS DSC L2b, and $\Delta\emptyset$ is the difference between RD (i.e., LOS CSK) and LOS DSC L2b; and for EGMS L3 as:

$$\left|\boldsymbol{P}_{RD}^{j,k}\right| = \left|\frac{\boldsymbol{P}_{L3}^{j,k} \cdot \boldsymbol{P}_{RD}}{\boldsymbol{P}_{RD} \cdot \boldsymbol{P}_{RD}}\ \boldsymbol{P}_{RD}\right| \tag{4}$$

where $(.)$ denotes the dot product between two vectors, $\boldsymbol{P}_{L3}^{j,k} = [P_{Up-do}^{j,k}\ , P_{East-West}^{j,k}]$, and $\boldsymbol{P}_{RD}$ can be defined as a unit vector along LOS CSK.

3.3 Fitting and Regression Analysis

After the compensation and projection steps, the time series of all three datasets are ready to be compared in terms of revealing the Displacement Velocity v and Thermal Expansion Coefficient α of each datapoint.

In order to obtain v, the mathematical model illustrated in Equation 5:

$$Def\ (t) = (\beta_1 + \beta_2\ t) + (\beta_3 \sin(\beta_2\ t)\ ) \tag{5}$$

is fitted to the Deformation [mm]–Time [year] data through a least square approach. The initial value of the coefficients is estimated through an iterative optimization process to minimize the Root Mean Square Error (RMSE) of the fitting. The sinusoidal part helps to account for the seasonality and to avoid the effect of this phenomenon on the linear deformation trend estimate. Figure 2 (a) shows the fitted model to the deformation time-series of a CSK datapoint P_{CSK} indicated in Figure 4 (a), as an example. To obtain the Thermal Expansion Coefficient α, a linear regression model is fitted to Deformation [mm]–Temperature [year] data (as an example, Figure 2 (b) for P_{CSK}). According to R^2 value, it can be seen that the variations in the deformation time-series show a reasonable linear correlation with the variations of temperature; demonstrating that target is getting away from the satellite by an increase in the temperature.

3.4 Comparison of Datasets

For comparing the datasets, the values of each parameter for each dataset are depicted along the bridge from one side to another side. Although the values obtained from the EGMS L3 dataset are shown at the location of the corresponding point, the values from EGMS L2b and CSK are spatially averaged based on some small overlapping envelopes along the length of the bridge. All the points, from each dataset, falling into an envelope are averaged and then the averaged value is shown for comparison. This downgrading of the sparse datapoints of EGMS L2b and CSK using these overlapping equally-distanced envelopes helps to have a smoother representation of parameter values along the bridge and forms a uniform auxiliary grid for downgrading.

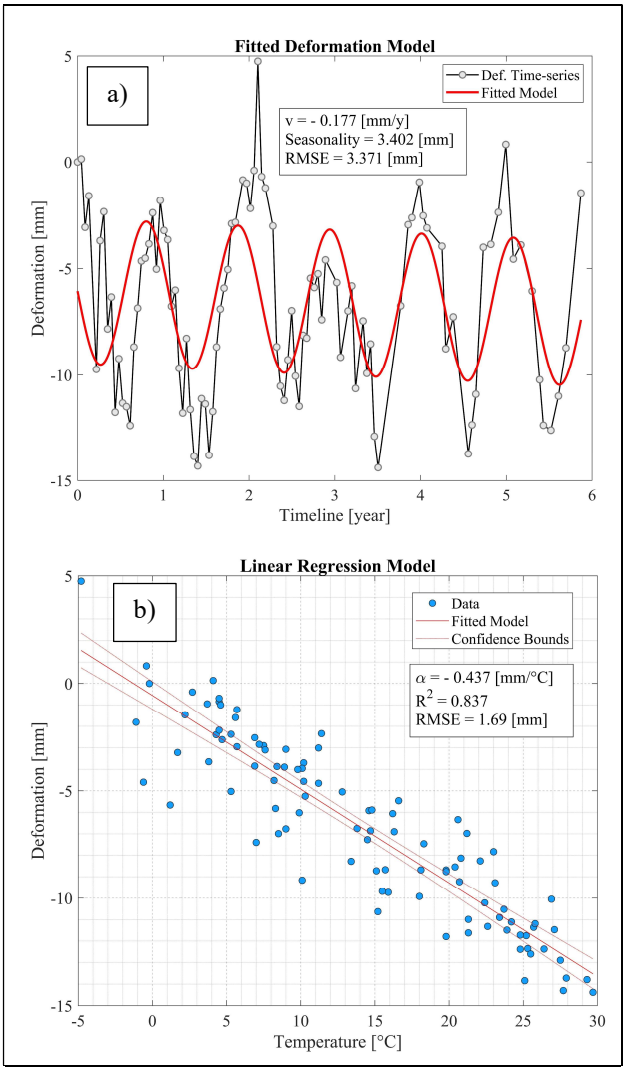

Figure 2. Fitted model on a) Deformation Time-series to obtain v, and b) Deformation Temperature-series to derive α

4. RESULTS AND DISCUSSION

In order to choose the suitable PSs in EGMS L2b and CSK datasets, thresholding the temporal coherence (γ_{temp}) value is performed. The threshold for EGMS L2b and CSK are set to be 0.50 and 0.70, respectively. Although for the CSK dataset, a high value of γ_{temp} is selected, there are several valuable EGMS L2b points with the γ_{temp} value between 0.50; Also, the CSK datasets are prepared through a non-linear InSAR analysis which often results in higher values of γ_{temp}. Therefore, this set of different γ_{temp} values are chosen for two datasets.

Figures 3 and 4 show the results of this study. In (a) sub-figures, the spatial distribution of CSK data points (coloured with the temporal coherence), EGMS L2b, and EGMS L3 points and the corresponding envelopes are shown. For Bridge 1, the whole length is perfectly covered by both CSK and EGMS L3 points, and some small portions are not covered by EGMS L2b. However, in the case of Bridge 2, EGMS L3 points are located close to the supports of the bridge, which does not allow unveiling of the differential behaviour between the midspan and the two supports of the bridge. As can be seen in Figure 4 (a), CSK points are not present at the midspan, since CSK PS candidates located at the midspan could not reveal the deformation time histories due to the strong fluctuations, and

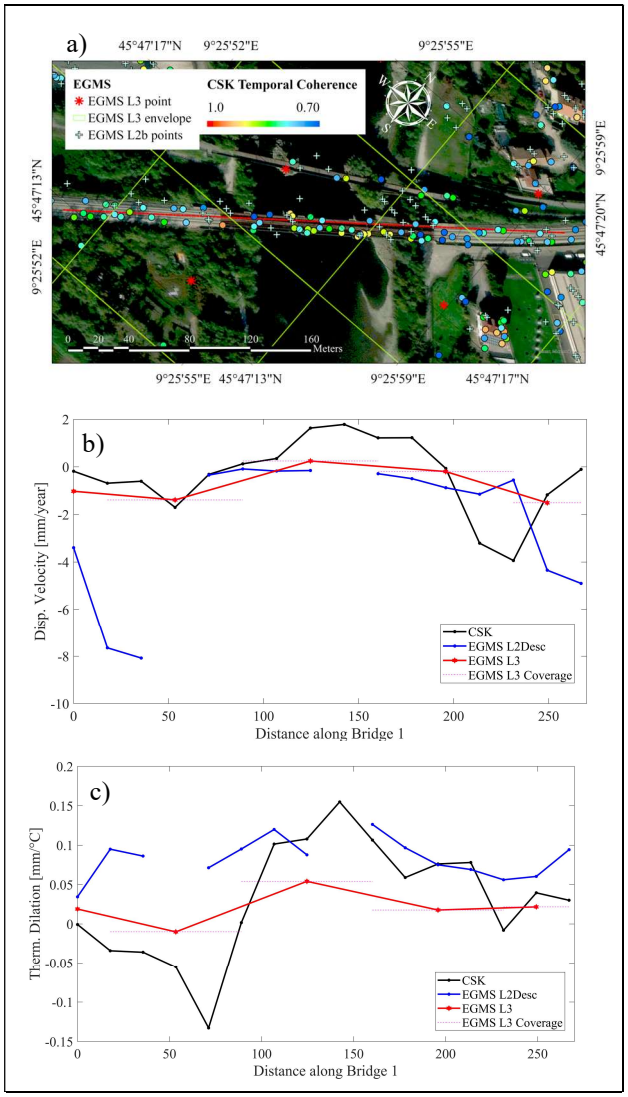

Figure 3. Bridge 1: a) EGMS and CSK data points, b) Displacement velocity, and c) Thermal dilation coefficient.

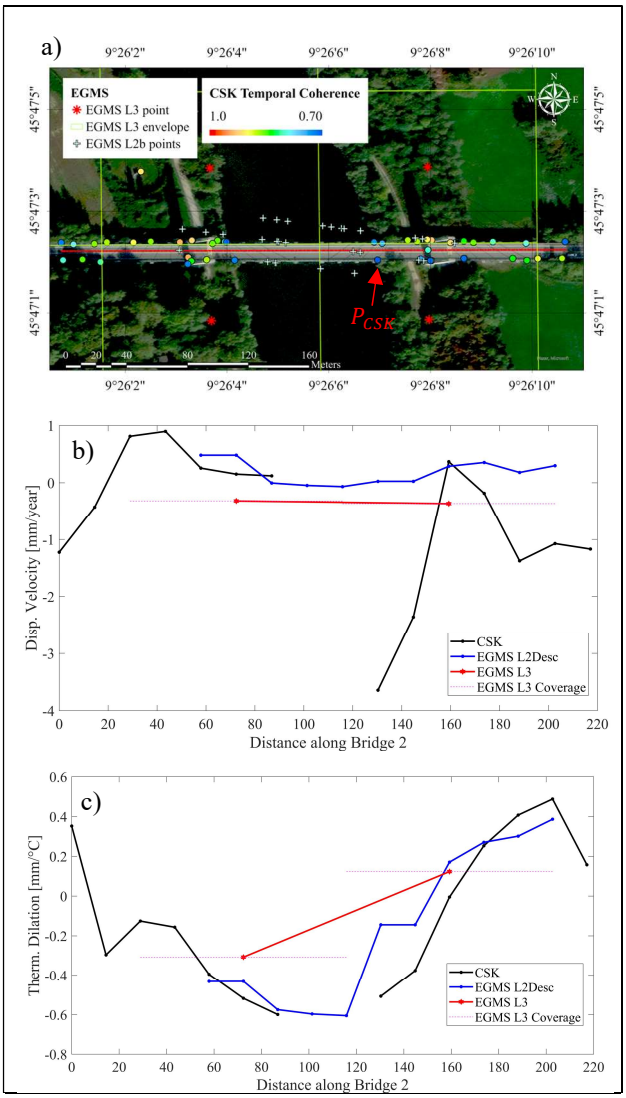

Figure 4. Bridge 2: a) EGMS and CSK data points, b) Displacement velocity, and c) Thermal dilation coefficient.

hence, the candidates are characterized by the high values of phase residuals (low temporal coherence) through InSAR processing. In this case, the points of EGMS L2b are well covering the midspan, however, these points do not show a suitable quality of geocoding. The points falling outside of the bridge show heights close to the real height of the bridge deck, and furthermore, the place where these points are settled is covered by water which is not expected to present a processed target. Therefore, it can be concluded that the sensed targets are related to the bridge.

According to the displacement velocities, the diagrams associated with CSK and both EGMS datasets show a reasonable consistency in terms of retrieving the trend from one side to the other side of Bridge 1 (differential settlements) and the close-to-stable situation of both sides of Bridge 2. Despite the consistency between displacement values coming from CSK and EGMS L3 datasets on the surrounding area located at the left side (minor settlement from the left side to the left-support) of Bridge 1, the information coming from EGMS L2b shows a greater settlement from the left side to the left-support. For Bridge 2, both EGMS datasets are showing a stable condition all along the bridge, however, the CSK dataset shows this stable condition only at the supports and reveals that the midspan is getting away from the satellite (negative values of velocity). This may be related to the non-linear InSAR analysis applied to CSK SAR images which could detect abnormalities in the deformation time history resulting in a negative value of displacement velocity.

In the case of the structural response of the bridges to the temperature variations, the lateral sides of Bridge 1 tend to have a stable (or slight lowering) behaviour, while the middle points tend to elevate along the LOS direction. This global variation is significantly unveiled by CSK and EGMS L3 datasets, however, due to a lack of datapoints in the EGMS L2b dataset of the left side and midspan of Bridge 1, this behaviour is only detected by this dataset on the right side of the bridge. Almost all the left and middle portion of Bridge 2 moves away from the satellite (more intensive at the midspan), however, the right part is going toward the satellite. There is an outstanding consistency between all the datasets in this case. The global behaviour is significantly revealed by EGMS L3, and the local differential variations are presented along Bridge 2 with a high level of agreement between CSK and EGMS L2b (where available).

Regarding the challenges and limitations of EGMS datasets for bridge monitoring, besides the low potential of EGMS-derived information in the detection of local differential behaviours along the width and height of the bridges (due to low spatial resolution of L3 and geocoding issues in L2b products), the magnitude of responses is slightly hammered down in EGMS L3 dataset.

Detection of deformation anomalies is found to be a limitation of both EGMS datasets, which keeps the importance of InSAR with high-resolution images through a reliable and case-specific approach (e.g., non-linear analysis). All these issues may be related to spatial insufficiency and the envelope-averaging procedure adopted for EGMS L3 time-series generation. The small discrepancies between CSK and L2b products may be related to the different InSAR algorithms which are adopted for processing.

In general, the consistency between CSK and EGMS measurements can be understood in both structural responses, again, more conveniently in terms of revealing the trend and global differential responses (in the case of EGMS L3) and partially in terms of local differential behaviour (in the case of EGMS L2b). Further investigation is required utilizing both ascending and descending CSK SAR images for vertical and horizontal deformation decomposition to be calibrated with GNSS data provided by the EGMS portal, to perform a better comparison between datasets, which is the goal for a future study.

5. CONCLUSIONS

This study is devoted to assessing the potential of the European Ground Motion Service (EGMS) for bridge monitoring. Two types of EGMS products are used: "Calibrated L2b" with Sentinel-1 spatial resolution and "Ortho L3" on a 100m uniform grid. A non-linear InSAR deformation analysis is performed on high-resolution Cosmo-SkyMed SAR images to obtain the deformation time series. The datasets, with different spatial and temporal resolutions, have been compared in terms of revealing displacement velocity and thermal expansion coefficient along two bridges in the north of Italy. The results showed that there is outstanding consistency between CSK and EGMS L3 products in detecting the global differential behaviour in both structural parameters. The consistency between the high-resolution CSK and the medium-resolution EGMS L2b-derived information showed that in most cases, the latter can be used to present both global and local differential variations of both parameters along both bridges. Although EGMS datasets showed some limitations (in comparison with CSK dataset) due to spatial insufficiency and being prepared through a different algorithm than the InSAR analysis performed in this study, this information provides an important opportunity for monitoring and condition assessment of bridges almost all over Europe.

6. ACKNOWLEDGEMENT

The authors would like to thank Dr. Perissin for providing the SARPROZ software package for SAR and InSAR processing of CSK SAR images. The authors express their gratitude to Italian Space Agency (ASI) for distributing Cosmo-SkyMed SAR images, and to EU Copernicus programme for free access on European Ground Motion Service (EGMS) and the valuable service products.

REFERENCES

Caspani, V., Tonelli, D., Rocca, A., Torboli, R., Vitti, A.,Zonta, D., 2023. Satellite InSAR technology for structural health monitoring of road bridges and the surrounding territory: a case study. Proceedings SPIE Sensors and Smart Structures Technologies for Civil, Mechanical, and Aerospace Systems, United States.

Costantini, M., Minati, F., Trillo, F., Ferretti, A., Passera, E., Rucci, A., Dehls, J., Larsen, Y., Marinkovic, P., Eineder, M., Brcic, R., Siegmund, R., Kotzerke, P., Kenyeres, A., Costantini, V., Proietti, S., Solari, L.,Andersen, H. S., 2022. EGMS: Europe-Wide Ground Motion Monitoring based on Full Resolution Insar Processing of All Sentinel-1 Acquisitions. Proceedings IGARSS 2022 - 2022 IEEE International Geoscience and Remote Sensing Symposium, 5093-5096.

Crosetto, M., Solari, L., Balasis-Levinsen, J., Casagli, N., Frei, M., Oyen, A.,Moldestad, D. A., 2020. Ground deformation monitoring at continental scale: the European ground motion service. The International Archives of Photogrammetry, Remote Sensing and Spatial Information Sciences, 43, 293-298.

Eskandari, R., 2022. Retrospective study of subsidence in Como town: integration of levelling measurements, DInSAR, and geospatial techniques. MSc thesis at Politecnico di Milano on civil Eng. for Risk Management, Lecco Campus (available online).

Eskandari, R., Scaioni, M., 2023a. RETROSPECTIVE STUDY OF VERTICAL GROUND DEFORMATION IN COMO, NORTHERN ITALY: INTEGRATION OF LEVELLING AND PSI MEASUREMENTS. Int. Arch. Photogramm. Remote Sens. Spatial Inf. Sci., XLVIII-4/W2-2022, 31-38.

Eskandari, R., Scaioni, M., 2023b. VALIDATION OF FULL-RESOLUTION DINSAR-DERIVED VERTICAL DISPLACEMENT IN CULTURAL HERITAGE MONITORING: INTEGRATION WITH GEODETIC LEVELLING MEASUREMENTS. ISPRS Ann. Photogramm. Remote Sens. Spatial Inf. Sci., X-M-1-2023, 79-86.

Eskandari, R., Scaioni, M., 2023c. VCWDtool: Weather Data Downloading and Visualizing in MATLAB. (Available online), (Last access July 2023).

Ferretti, A., Passera, E.,Capes, R., 2021. Algorithm Theoretical Basis Document. EGMS Documentation, (Available online).

Ferretti, A., Prati, C., Rocca, F. J. I. T. o. g.,sensing, r., 2000. Nonlinear subsidence rate estimation using permanent scatterers in differential SAR interferometry. 38, 2202-2212.

Gagliardi, V., Tosti, F., Ciampoli, L. B., Battagliere, M. L., Tapete, D., Amico, F. D., Threader, S., Alani, A. M.,Benedetto, A., Spaceborne Remote Sensing for Transport Infrastructure Monitoring: A Case Study of the Rochester Bridge, UK. Proceedings, IGARSS 2022 - 2022 IEEE International Geoscience and Remote Sensing Symposium, 4762-4765.

Gawronek, P.,Makuch, M., 2019. TLS Measurement during Static Load Testing of a Railway Bridge. ISPRS Int. J. Geo-Inf, 8, 44.

Kotzerke, P., Siegmund, R.,Langenwalter, J., 2022. Product User Manual. EGMS Documentation, (Available online).

Lazecky, M., Perissin, D., Bakon, M., Sousa, J. M. d., Hlavacova, I.,Real, N., Potential of satellite InSAR techniques for monitoring of bridge deformations. Proceedings, 2015 Joint Urban Remote Sensing Event (JURSE), 1-4.

Lazecký, M., Rapant, P., Perissin, D.,Bakoň, M., 2014. Deformations of Highway over Undermined Ostrava-Svinov Area Monitored by InSAR Using Limited Set of SAR Images. Procedia Technology, 16, 414-421.

Macchiarulo, V., Milillo, P., Blenkinsopp, C.,Giardina, G., 2022a. Monitoring deformations of infrastructure networks: A fully automated GIS integration and analysis of InSAR time-series. 21, 1849-1878.

Macchiarulo, V., Milillo, P., Blenkinsopp, C., Reale, C.,Giardina, G., 2022b. Multi-temporal InSAR for transport infrastructure monitoring: recent trends and challenges. Proceedings of the Institution of Civil Engineers – Bridge Engineering, 1-26.

Mayunga, S. D., Bakaone, M. J. J. o. D. A.,Processing, I., 2021. Dynamic deformation monitoring of lotsane bridge using global positioning systems (GPS) and linear variable differential transducers (LVDT). 9, 30-50.

Nappo, N., Ferrario, M. F., Livio, F.,Michetti, A. M., 2020. Regression Analysis of Subsidence in the Como Basin (Northern Italy): New Insights on Natural and Anthropic Drivers from InSAR Data. 12, 2931.

Perissin, D., Wang, Z.,Wang, T. J. P. o. t. I., Sidney, Australia, 2011. The SARPROZ InSAR tool for urban subsidence/manmade structure stability monitoring in China. 1015.

Poreh, D., Iodice, A., Riccio, D.,Ruello, G. J. E. J. o. R. S., 2016. Railways' stability observed in Campania (Italy) by InSAR data. 49, 417-431.

Selvakumaran, S., Rossi, C., Barton, E.,Middleton, C. R., 2021. Interferometric Synthetic Aperture Radar (InSAR) in the Context of Bridge Monitoring. Advances in Remote Sensing for Infrastructure Monitoring, 183-209.

Sun, L., Shang, Z., Xia, Y., Bhowmick, S.,Nagarajaiah, S., 2020. Review of Bridge Structural Health Monitoring Aided by Big Data and Artificial Intelligence: From Condition Assessment to Damage Detection. Journal of Structural Engineering, 146, 04020073.

Tang, Q., Xin, J., Jiang, Y., Zhou, J., Li, S.,Chen, Z., 2022. Novel identification technique of moving loads using the random response power spectral density and deep transfer learning. Measurement, 195, 111120.

Wang, X., Zhao, Q., Xi, R., Li, C., Li, G.,Li, L., 2021. Review of Bridge Structural Health Monitoring Based on GNSS: From Displacement Monitoring to Dynamic Characteristic Identification. IEEE Access, 9, 80043-80065.

Xi, R., He, Q.,Meng, X., 2021. Bridge monitoring using multi-GNSS observations with high cutoff elevations: A case study. Measurement, 168, 108303.

Zainon, O.,Fong Kian, S., 2021. Monitoring Of Concrete Bridge Using Robotic Total Station. Journal of Advanced Geospatial Science & Technology, 1, 163-192.

Zarate Garnica, G. I., Lantsoght, E. O. L.,Yang, Y., 2022. Monitoring structural responses during load testing of reinforced concrete bridges: a review. Structure and Infrastructure Engineering, 18, 1558-1580.